

## Decarbonization Reactions between Sodium Metaborate and Sodium Carbonate

Zaki Yusuf and John Cameron\*

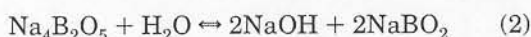
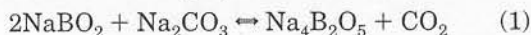
Department of Paper and Chemical Engineering, Western Michigan University, Kalamazoo, Michigan 49008

Autocausticizing, used for the recovery of kraft pulping chemicals, is nearing commercialization. This technology produces sodium hydroxide directly on dissolving the molten salts produced in the kraft recovery furnace in water. Thus, the dependence on the lime cycle for sodium hydroxide is reduced. Ongoing trials in several kraft mills are in progress to implement this technology. In this study, the reactions between sodium metaborate ( $\text{NaBO}_2$ ) and sodium carbonate ( $\text{Na}_2\text{CO}_3$ )—the anticipated reactants—were studied in a tubular reactor heated in an electric furnace. It was found that the reaction begins in the solid phase, followed by a liquid phase reaction. The reaction rate is extremely rapid once the system melts. It was proposed that these reactions could proceed through the intermediate formation of sodium diborate ( $\text{Na}_4\text{B}_2\text{O}_5$ ).

### Introduction

Sodium hydroxide ( $\text{NaOH}$ ) and sodium sulfide ( $\text{Na}_2\text{S}$ ) are the two principal pulping chemicals used in the kraft process. After evaporation, the spent liquor from the pulping process is sent to the recovery boiler furnace to generate energy and to recover the pulping chemicals. In this process, the recovery boiler serves as both a chemical reactor and a steam boiler. It produces steam from the energy liberated during the combustion of organic components of black liquor. The inorganic matter in kraft black liquor consists mainly of sodium carbonate, sodium sulfide, sodium thiosulfate, sodium sulfate, and sodium salts of organic acids.<sup>1</sup> In the kraft furnace, the inorganic compounds from the pulping reaction are converted primarily to sodium sulfide and sodium carbonate. The lime cycle then converts the sodium carbonate back into the sodium hydroxide, one of the active pulping chemicals.

In the late 1970s, Janson<sup>2–6</sup> was searching for chemicals that would act as autocausticizing agents for decarbonizing sodium carbonate in the kraft furnace and generate sodium hydroxide on dissolution in the green-liquor dissolving tank. Several inorganic salts were evaluated, including sodium tetraborate ( $\text{Na}_2\text{B}_4\text{O}_7$ ), sodium metaborate ( $\text{NaBO}_2$ ), sodium diphosphate ( $\text{Na}_4\text{P}_2\text{O}_7$ ), sodium silicate ( $\text{Na}_2\text{Si}_2\text{O}_7$ ), and alumina ( $\text{Al}_2\text{O}_3$ ), as potential autocausticizing agents. He recognized that sodium aluminate and sodium silicate would cause major process instability in the kraft pulping system. He also acknowledged that sodium metaborate seemed very weakly alkaline and was more suitable for alkaline bleaching, although it was agreed that  $\text{Na}_4\text{B}_2\text{O}_5$  might act as an effective causticizing agent.<sup>4,5</sup> The following equations for the autocausticizing reaction were proposed by Janson when sodium borate really was used as autocausticizing agent.<sup>6</sup>

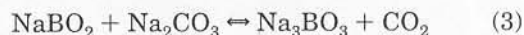


Additionally, he recognized that the decarbonization reaction 1 is reversible in nature, but he could not

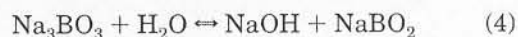
clearly confirm whether reaction 2 goes to completion. He further acknowledged that when borate salts go into solution they demonstrate complicated solution chemistry. He also agreed with Ingrid<sup>7</sup> that  $\text{B}(\text{OH})_4^-$  is the dominant species above pH 10.5–11.0. Maeda<sup>8</sup> and Maya<sup>9</sup> on the basis of Raman spectroscopic studies independently concluded that  $\text{B}(\text{OH})_4^-$  is the major borate ion at high alkalinity. Salentine<sup>10</sup> using NMR studies has also identified the presence of  $\text{B}(\text{OH})_4^-$  ions in aqueous system.

Grace cautioned,<sup>11</sup> on the basis of the stoichiometry (reaction 1) proposed by Janson, that the introduction of metaborate as an autocausticizing agent in kraft pulping would double the inorganic deadload of black liquor. This would result in higher energy consumption for fluid moving devices, lower heating value per unit mass, and higher sensible heat load during both the evaporation and the combustion of the resulting black liquor. This finding made the feasibility of using borate in conventional kraft pulping less attractive.

A major breakthrough came in the 1990s when Tran et al.<sup>12</sup> corrected the stoichiometry associated with reaction 1 and proposed the following:



This new finding rejuvenated the borate-based kraft pulping research because reaction 3 shows that the metaborate requirement is half that proposed by Janson. They further added that on dissolving the trisodium borate salt reacts with water to form sodium hydroxide and regenerate sodium metaborate, given by the following reaction:<sup>12</sup>



It should be pointed out that the temperature in the recovery boiler ranges from 850 °C to as high as 1250 °C.<sup>1</sup> Therefore, the feasibility of sodium borate(s) as decarbonization agents in the chemical recovery boiler largely depends on understanding the stoichiometry and rate-controlling parameters of reaction 3 in that temperature interval. The commercial viability of using sodium borates as a decarbonizing agent during the burning of black liquor in the recovery boiler furnace

\* To whom correspondence should be addressed.

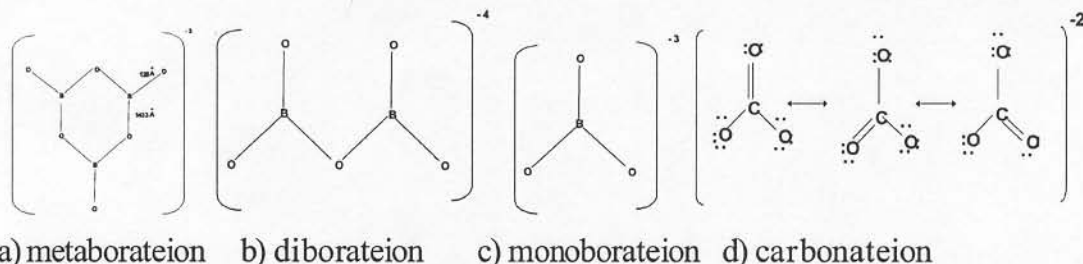
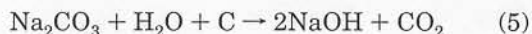


Figure 1. Structures of metaborate, diborate, monoborate, and carbonate ions.

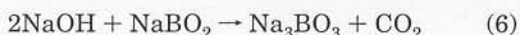
depends on various factors. These include the combustion process in the char/smelt bed, the temperature, inorganic and organic constituents, and CO/CO<sub>2</sub> concentrations in the surroundings.

If reaction 3 is reversible, the final conversion could depend on both the rate and equilibrium of the reaction. Because of the high level of carbon present in the char bed of the kraft furnace, any carbon dioxide formed is converted to carbon monoxide, which shifts the equilibrium of reaction 3 toward the right and completion.

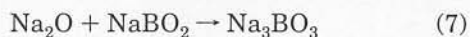
Tran et al.<sup>13</sup> have expressed a concern that the reaction between carbonate and metaborate may be slow and suggested that the conversion rate is faster in the mill trials because the reaction may follow several different pathways. They proposed that near the char bed, under strong reducing atmosphere and high temperature, sodium carbonate might react with carbon and water vapor to form sodium hydroxide. The following equation was proposed for such a reaction:



It was also proposed that sodium hydroxide produced from reaction 5 reacts with sodium metaborate to form trisodium borate given by the following equation:



Additionally, they also proposed that sodium oxide formed from the reaction between sodium vapor and oxygen also reacts with sodium metaborate to form trisodium borate given by the following equation:



Finally, they suggested that since reaction 6 occurs at a lower temperature it is likely to be the main pathway for trisodium borate formation in the recovery boiler.

The structures of metaborate, diborate, monoborate, and carbonate<sup>14,15</sup> ions are shown in Figure 1. All three above-mentioned borates contain trigonal BO<sub>3</sub> group; however, a tetrahedral BO<sub>4</sub> group is also present in tetraborate in addition to a BO<sub>3</sub> group. Sodium metaborate (NaBO<sub>2</sub>) is essentially a cyclic compound with a melting point of 966 °C.<sup>16,17</sup> Sodium pyroborate (Na<sub>4</sub>B<sub>2</sub>O<sub>5</sub>) is diborate in structure and remains as condensed ions.<sup>14</sup> Sodium diborate has a melting point of 625 °C.<sup>18</sup> Trisodium borate has a monoborate structure<sup>14</sup> with an unknown melting point.

### Objectives of the Study

The primary objective of this study is to provide information on the stoichiometry and effect of the rate-controlling parameters on the decarbonization reaction between sodium metaborate and sodium carbonate.

Because this reaction occurs at high temperatures and involves multiple phases, little information is available concerning its nature or rate-controlling parameters.

One specific objective of this study is to verify the stoichiometry proposed by Tran et al.<sup>12</sup> of the decarbonization reaction between sodium carbonate and sodium metaborate in the molten state. Although Tran et al. proposed the corrected stoichiometry for this reaction, no data were presented to confirm this stoichiometry and little information was provided concerning the rate-controlling parameters. Another objective of this study is to determine the effect of the rate-controlling parameters, such as temperature, on the reaction. A third objective of this study is to determine if any reaction occurs between sodium metaborate and sodium carbonate below the melting points of the reactants. The final objective of the study is to identify the governing parameters that control the conversion rate of this reaction.

It should be pointed out that it is beyond the scope of the current study to determine the mechanistic steps that are involved in the decarbonization reactions. The experimental plan consisted of studying the reaction between sodium metaborate and sodium carbonate at various molar ratios, from low temperature to temperature above the salt mixture's pooled melting point.

### Experimental Section

**Salt Preparation.** To ensure good mixing between the reactants, different ratios of reagent grade sodium metaborate to sodium carbonate were prepared by dissolving sodium carbonate and sodium metaborate in deionized water and drying the solution at 110–120 °C. The dried salt was then ground to powder and mixed.

**Experimental System.** The experimental system used in this study is shown in Figure 2. The experimental system consists of an alumina reactor (Coors Tek AD-998) heated by a circular electric furnace, mass flow meter, carbon dioxide/carbon monoxide analyzer, and data acquisition system. After the mixed salts were placed in the alumina crucible, the salts were heated and sweep gas (nitrogen) was passed through the reactor. A mass flow meter (Omega FMA-1900) was used to monitor the sweep gas flow rate. The composition of the off-gas (product) was measured with an infrared gas analyzer (MEXA-554 JU (Horiba) gas analyzer). The reaction rate was then followed using a material balance on the system. The temperature of the salt mixture was measured with a K-type thermocouple (Medtherm). The sweep gas flow rate, system temperature, and off-gas composition were continuously monitored and recorded using a computer and data acquisition system (Measurement Computing Corp., Middleboro,

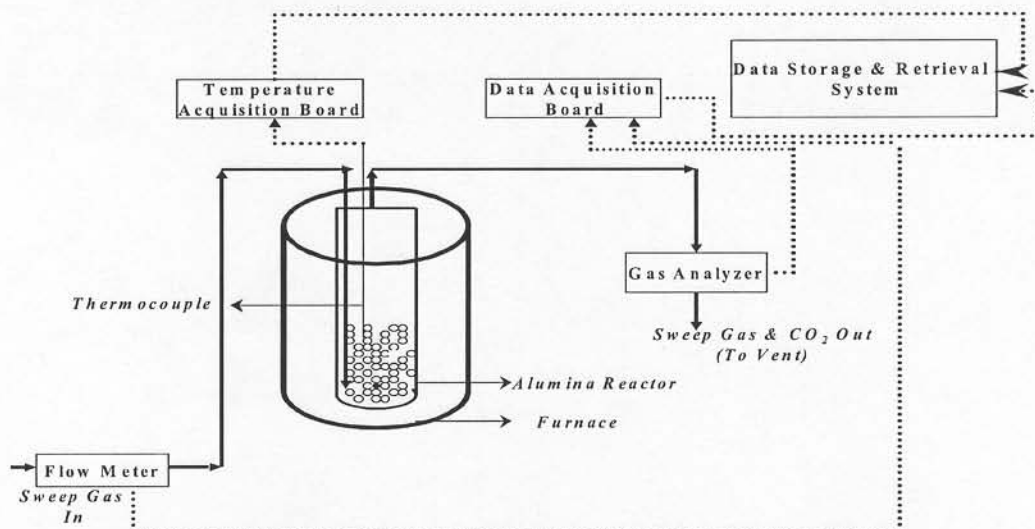


Figure 2. Experimental system showing alumina reactor, thermocouple, electric furnace, gas flow meter, gas analyzer, and data acquisition system.

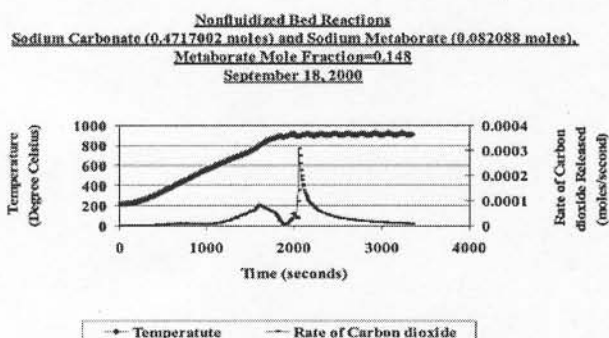


Figure 3. Carbon dioxide generation rate and temperature versus time.

MA). The data were recorded every 2 s into an Excel (MS Office 97) spreadsheet and continuously integrated (with respect to time) to determine the total amount of product gas (carbon dioxide) produced.

The melting point of the salt mixture was evident by a rapid increase in reaction rate often accompanied by an inflection point on the temperature versus time curve and a bubbling sound. In the initial experiments, it was observed that the reaction began before the salts melted. To confirm this solid phase reaction, in the later experiments, the temperature of the system was held for a long period at a constant temperature below the melting point, until the generation of the product gases ceased.

## Results and Discussion

In the initial experiments, the reaction mixture was gradually heated and the product gas continuously analyzed. It was observed during the initial experiments that carbon dioxide was the only product gas from the reaction. Data obtained during these initial experiments are shown in Figures 3 and 4. Figure 3 shows the product gas generation rate and temperature versus time, while Figure 4 shows the cumulative carbon dioxide versus time. Both solid and molten-state reactions can be followed from these graphical representations. The first peak in Figure 3 signifies the maximum carbon dioxide generation rate in the solid phase. This

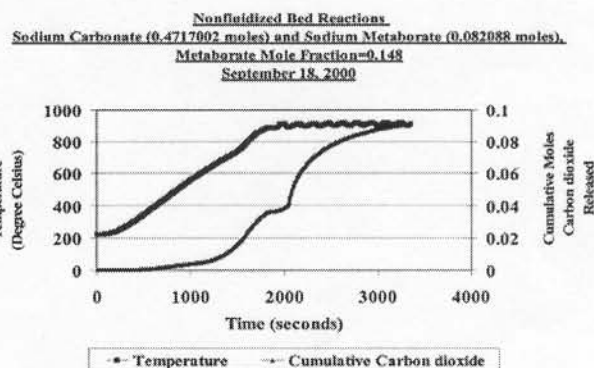


Figure 4. Cumulative carbon dioxide and temperature versus time.

rate of carbon dioxide declined asymptotically to non-detectable level despite the existence of nonequilibrium conditions existing due to the continuous flow of the sweep gas. The formation of reaction product along the reaction front and the immobility of the reactants in the solid state could have resulted in the cessation of the solid phase reaction. The second peak is observed after the system melted. As the salt mixture melted, a sudden release of carbon dioxide is evident from the sharp and large second peak. This could result from the increased reactant mobility in the molten phase.

One of the surprising findings from these initial experiments is that the reaction begins around 600 °C, which is well below the melting point of the individual reactants (the melting points of sodium carbonate and sodium metaborate are 851 and 966 °C, respectively). As the temperature of the furnace was gradually increased, the rate of carbon dioxide generation increased during the solid phase reaction until a maximum point was reached and gradually decreased and finally ceased before the salt mixture reached its melting point. A sharp increase in the carbon dioxide generation rate was observed as the reaction mixture melted normally between 850 and 900 °C. The reaction was continued until the carbon dioxide generation ceased.

In the later experiments, to determine the extent of the reaction in the solid phase, the system was heated

Table 1. Reaction Conditions and Results with Respect to Carbon Dioxide Generation during Solid Phase Reaction

date	temp of reaction to mp, °C	initial reactants, mol		mole fraction metaborate	cumul solid phase CO <sub>2</sub> produced, mol	% metaborate conversion in terms of reaction 3
		sodium carbonate	sodium metaborate			
18-Sep-00	892	0.472	0.082	0.148	0.040	48.780
19-Oct-00	909	0.426	0.038	0.081	0.025	66.310
24-Oct-00	815	0.472	0.189	0.286	0.054	28.560
28-Oct-00 <sup>a</sup>		0.485	0.095	0.164		
13-Dec-00	907	0.436	0.041	0.086	0.020	49.030
14-Dec-00	902	0.424	0.040	0.086	0.020	49.260
20-Dec-00	880	0.467	0.100	0.176	0.041	41.040
23-Dec-00	875	0.459	0.100	0.178	0.044	44.250
26-Dec-00	860	0.466	0.101	0.178	0.041	40.760
27-Oct-01	820	0.527	0.075	0.124	0.025	33.780
average						44.641
std dev						10.794

<sup>a</sup> The purge tube end was placed above the salt mixture.

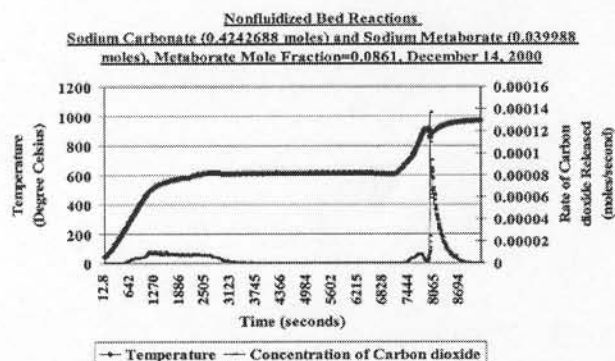


Figure 5. Carbon dioxide generation rate and temperature versus time.

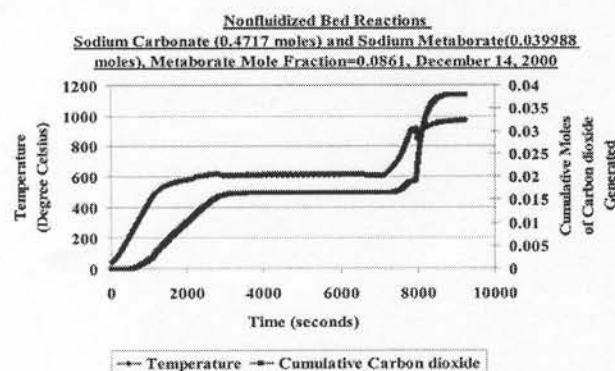


Figure 6. Cumulative carbon dioxide and temperature versus time.

to a point where carbon dioxide was evolved but below the system's melting point. The temperature was then held constant and the reaction allowed to continue until the generation of carbon dioxide ceased. At this point, the system's temperature was again increased. Once the temperature began to increase, the generation of carbon dioxide commenced again.

**Extent of Reaction in the Solid Phase.** To determine the effect of the sodium metaborate to sodium carbonate ratio on the reaction rate and extent of the reaction in the solid phase, the reactions were studied at different sodium metaborate to sodium carbonate ratios. The experiments conducted in this phase are shown in Table 1. One such experimental result is also shown in Figures 5 and 6. These figures show that the generation of carbon dioxide begins at about 600 °C. The reaction continues as the temperature of the system is

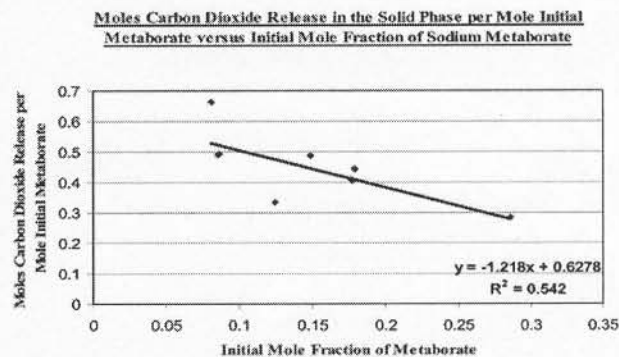


Figure 7. Effect of initial mole fraction of sodium metaborate on carbon dioxide generation in the solid phase.

held at 728 °C (well below the melting point of both reactants), but eventually ceases. In this case, it could be observed that approximately 50% of the metaborate was converted—based on reaction 3—during the solid phase reaction. Although the release of carbon dioxide during the solid phase reaction ceased at a given temperature, the reaction started again as soon as the temperature was further increased.

It was observed during the solid-state reaction that (44.64 ± 10.79)% of the total metaborate reacted based on the stoichiometry shown in reaction 3. Additionally, Figure 7 shows that, as the mole fraction of sodium metaborate was increased, there was a tendency for the percentage of conversion to decrease during the solid phase reaction. This suggests that there is a possibility of forming either all sodium diborate or a mixture of both sodium diborate and trisodium borate. These compounds were indicated by the phase diagrams published by Tran et al.<sup>12</sup>

**Molten Phase Reaction and Stoichiometry.** Once the solid phase reaction ceased, the temperature of the system was increased again. Immediate evolution of carbon dioxide was noticed followed by the complete termination in some cases, and for other cases considerable decline of the reaction rate was observed, as the temperature approached the melting point. Such a phenomenon may be attributed to either the rearrangement of the molecules or the shift in reaction mechanisms, or both. Subsequently, for all cases, as the salt mixture reached its pooled melting point, a vigorous increase in the rate of carbon dioxide evolution was observed. It is also observed from Table 2 that the melting point of the salt mixture tended to decrease with increasing mole fraction of metaborate. The variation

Table 2. Reaction Conditions and Results with Respect to Carbon Dioxide Generation for Molten Phase Reaction

date	pooled mp, °C	avg molten phase reaction temp, °C (approx)	initial reactants, mol		mole fraction metaborate	cumul molten phase CO <sub>2</sub> produced, mol	% metaborate conversion in terms of reaction 3
			sodium carbonate	sodium metaborate			
18-Sep-00	892	910	0.472	0.082	0.148	0.084	97.671
19-Oct-00	909	1050	0.426	0.038	0.081	0.036	103.506
24-Oct-00 <sup>a</sup>	815	976	0.472	0.189	0.286	0.16622 <sup>a</sup>	
28-Oct-00 <sup>b</sup>		1055	0.485	0.095	0.164		
13-Dec-00	907	1000	0.436	0.041	0.086	0.036	111.218
14-Dec-00	902	950	0.424	0.040	0.086	0.035	111.924
20-Dec-00	880	910	0.467	0.100	0.176	0.101	98.990
23-Dec-00	875	920	0.459	0.100	0.178	0.101	98.265
27-Oct-01	820	1000	0.527	0.075	0.124	0.071	104.654
average							103.613
std dev							5.960

<sup>a</sup> Reaction was stopped before completion. <sup>b</sup> The purge tube end was placed above the salt mixture.

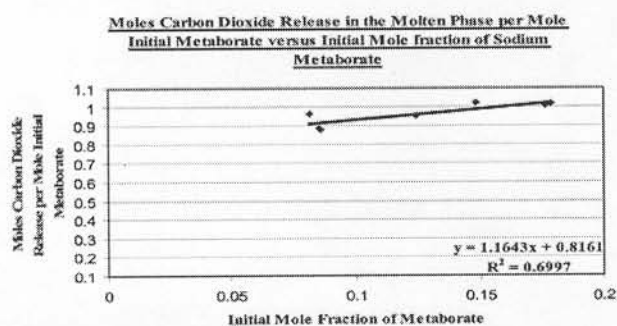


Figure 8. Effect of sodium metaborate level on moles of carbon dioxide released per mole initial metaborate.

of melting point of the mixture did show anomalous behavior, signifying a complex relationship with the heat of reaction, mole fraction of the initial reactants, and intermediate product.

Tran et al.<sup>12</sup> proposed that the decarbonization reaction follows reaction 3, which implies that 1 mol of sodium metaborate reacts with 1 mol of sodium carbonate resulting in the release of 1 mol of carbon dioxide. The results, in this particular case (Figure 6), show that complete conversion of initial reactant (sodium metaborate) was achieved in terms of carbon dioxide generated, which confirms reaction 3. The results for the molten phase reactions, reaction temperatures, and amount of reactants are shown in Table 2 and Figure 8. Here, the data shown in Table 2 reveal that 1 mol of carbon dioxide is released per mole of sodium metaborate reacted (reaction 3) rather than 1/2 mol of carbon dioxide released per mole of sodium metaborate originally proposed by Janson (reaction 1). These results as evident from Table 2 and Figure 8 confirm the stoichiometry proposed by Tran et al.<sup>12</sup> The average (103%) and standard deviation (5.9%) of the percent conversion, achieved from reaction 3, are also shown in Table 2. Moreover, it could be also observed by comparing all the other results that the solid-state rate of reactions was very slow compared to the rate of molten phase reactions irrespective of the (higher/lower) mole fraction of metaborate. It could be also observed that the solid phase reactions were about an order of magnitude slower than the molten phase reactions for all cases. The results also show that the reaction is extremely rapid above its melting point and goes to completion in about 10–15 min once the system melts.

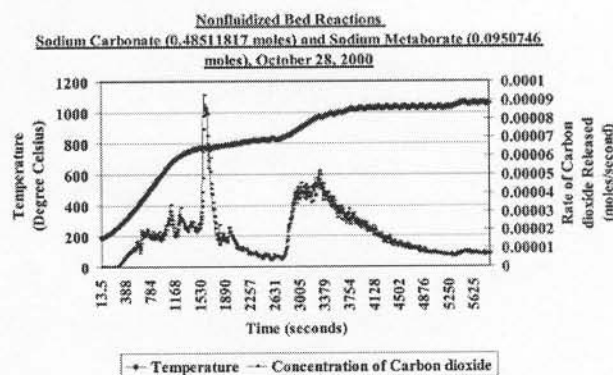


Figure 9. Rate of carbon dioxide generation and temperature versus time.

### Implications in Chemical Recovery Boiler

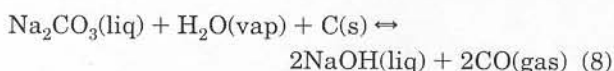
It was observed from the results that the reaction takes place in both the solid phase and molten phase. Once the system melts, the reaction is extremely rapid. However, it should be pointed out that inefficient removal of carbon dioxide could markedly reduce the rate of reaction. This was observed when the purge tube was placed above the salt mixture. Here, the carbon dioxide was not effectively removed, which significantly decreased the reaction rate, although the flow rate of the sweep gas was maintained in the range of ~6 L/min as in other cases. The carbon dioxide generation rate from this experimental arrangement is shown in Figure 9. This suggests that reaction 3 is reversible in nature and that for this reaction to go to completion the carbon dioxide must be removed. This is a critical finding of the study since it provides evidence that, even if the reactant mixture is well past its pooled melting point, reaction 3 may only reach a dynamic equilibrium at any temperature unless carbon dioxide released from the reaction is completely swept away from the reactant mixture or converted to other reaction product(s). This implies that the reaction rate and conversion would decrease in the recovery boiler if the carbon dioxide level increases. However, it should be pointed out that the presence of carbon on the smelt bed should act as a sink for carbon dioxide by converting it to carbon monoxide and thus increasing the rate and extent of conversion. This phenomenon may occur because the char or carbonaceous matter present in the char bed of the recovery boiler generally converts the carbon dioxide to carbon monoxide in this reducing atmosphere.<sup>20</sup> It also implies that such a reaction is more feasible in the reducing

Table 3. Gibbs Free Energy Change of Reaction 5 at Various Temperatures

temp, °C	Gibbs free energy of formation, kJ/mol					approx Gibbs free energy change for reaction 8, kJ/mol
	sodium carbonate (liq)	carbon (solid)	water (vapor)	sodium hydroxide (liq)	carbon monoxide (gas)	
727	-850.159	0	-192.59	-282.478	-200.275	77.243
1027	-760.294	0	-175.774	-236.877	-226.509	9.296
1227	-684.221	0	-164.376	-198.087	-243.74	-35.057

zone of the recovery boiler. Since the surface of the smelt bed temperature ranges from 900 to 1100 °C, reaction 3 is viable in the recovery boiler and the rate would be governed by conversion of carbon dioxide to carbon monoxide.

Tran et al.<sup>13</sup> proposed a different reaction pathway for the rapid formation of trisodium borate based on reaction 5. However, when reaction 5 was examined it was observed that the reaction stoichiometry was not balanced. The corrected stoichiometry is given by the following:



The feasibility of reaction 8 was investigated by computing the Gibbs free energy change at various temperatures using data obtained from NIST-JANAF Thermochemical tables,<sup>19</sup> and the results of these calculations are shown in Table 3.

Interpolation of the above data shows that the change in Gibbs free energy is 0 at approximately 1070 °C. Although  $\Delta G_R \approx -35$  kJ/mol for reaction 8 at 1227 °C, suggesting that reaction 8 is favorable above 1070 °C, the large levels of carbon monoxide in the vicinity of the char bed should suppress reaction 8. Additionally, since the maximum surface temperature of the char bed is between 900 and 1100 °C,<sup>20</sup> any sodium hydroxide present below the surface of the char bed would tend to convert back to sodium carbonate as the temperature falls below 1070 °C due to the thermodynamic constraint (positive Gibbs free energy change). Therefore, the reaction pathways (reactions 5 and 6 or 8) proposed by Tran et al.<sup>13</sup> is only possible if the temperature is above 1070 °C and the carbon monoxide concentration is negligible near the vicinity of the reaction. On the contrary, the carbon monoxide concentration is large near the vicinity of the char bed and there exists a decreasing temperature gradient from its surface (~1100 °C) to its bottom (~760 °C). Therefore, it is proposed that the major conversion to trisodium borate within the char bed would follow reaction 3 when the carbon monoxide concentration near the surroundings and the temperature profile of the bed are considered.

The implication of the decarbonization reaction 3 with sodium metaborate is that it begins at low temperatures (~600 °C), in the solid state, and may be viable in the black liquor gasification processes. Several gasification processes with more efficient energy recovery have been proposed with operating temperatures between 600 and 1000 °C.<sup>21</sup> At 600 °C, some conversion of the metaborate would be expected to occur in a solid phase reaction. At 1000 °C, most of the metaborate should be converted to trisodium borate since the reaction occurs in a reducing environment.<sup>22</sup> However, it should be mentioned that hydrogen sulfide is formed during black liquor gasification processes, which demands scrubbing of product gases, by sodium hydroxide. Trisodium borate, which naturally produces caustic upon hydrolysis, should

reduce additional caustic demand in such a process. However, additional research is needed to determine the feasibility of the decarbonization reaction during the black liquor gasification.

Determination of the activation energy for these reactions is difficult due to the following: (a) there are multiple reactions occurring (solid and liquid phase), (b) the reaction appears to be reversible when carbon dioxide is not continuously swept away from the reactor, and (c) when the temperature reaches a steady state and the system is fully melted, a substantial amount of the metaborate has already reacted with carbonate and only a small fraction of metaborate remains in the system. Thus determination of the exact amount of metaborate present becomes difficult, which, in turn, makes the estimation of activation energy difficult. Moreover, the probability of sodium diborate formation during the solid phase reaction along with unreacted sodium metaborate may have resulted in two parallel reactions, which, in turn, create problems in separating the variables from these two parallel reactions to obtain the reaction orders, preexponential constant, and activation energy from a nonlinear fit. In such a situation, it is essential to separate these two convoluted reactions by simultaneously collecting the real-time concentration of sodium diborate and sodium metaborate. However, the detection of sodium diborate concentration could not be realized due to the unavailability or limitation of the experimental setup.

## Conclusions

(a) A major finding in this study is that reaction 3 starts in the solid phase (~600 °C) and a considerable amount of metaborate reacts before melting occurs. There is a strong indication that the resulting borate salt product is a mixture of trisodium borate and sodium diborate.

(b) Reaction 3 is rapid immediately upon melting (~850 °C) and can easily account for the higher rate of reaction as evident during the mill trials; no additional reaction mechanism is required to support the high rate of reaction.

(c) The extent of the conversion reaction 3 is governed by the effective removal of carbon dioxide from the system.

(d) For the solid-state reactions, the extent of conversion varied in the opposite direction with respect to the increase in mole fraction of sodium metaborate.

(e) The stoichiometry of the reaction between sodium metaborate and sodium carbonate has been reconfirmed (reaction 3).

## Literature Cited

- Grace, T. M.; Malcolm, E. W. *Pulp and Paper Manufacture; Alkaline Pulp* The Joint Textbook Committee of the Paper Industry, TAPPI: Atlanta, 1989; Vol. 5.
- Janson, J. The use of unconventional alkali in cooking and bleaching—Part 1. A new approach to liquor generation and alkalinity. *Pap. Puu* 1977, 59 (6–7), 425–430.

- (3) Janson, J.; Pekkala, O. The use of unconventional alkali in cooking and bleaching—Part 2; Alkali cooking of wood with the use of borate. *Pap. Puu* **1977**, *59* (9), 546–557.
- (4) Janson, J. The use of unconventional alkali in cooking and bleaching—Part 4. Alkali cooking of wood with the use of borate. *Pap. Puu* **1978**, *60* (5), 349–357.
- (5) Janson, J. The use of unconventional alkali in cooking and bleaching—Part 5. Autoausticizing reactions. *Pap. Puu* **1979**, *61* (1), 20–30.
- (6) Janson, J. The conventional use of unconventional alkali in cooking and bleaching—Part 6. Autoausticizing of sulphur-containing model mixtures and spent liquors. *Pap. Puu* **1979**, *61* (2) 98.
- (7) Ingri, N. Equilibrium Studies of Polyanions. 2. Polyborates in NaClO<sub>4</sub> Medium. *Acta Chem. Scand.* **1957**, *11* (6), 1034.
- (8) Maeda, M.; Hirao, T.; Kotaka, M.; Kakihana, H. Raman spectra of polyborate ions in aqueous solution. *J. Inorg. Nucl. Chem.* **1979**, *41*, 1217.
- (9) Maya, L. Identification of Polyborate and Fluoropolyborate Ions in Solution by Raman Spectroscopy. *Inorg. Chem.* **1976**, *15* (9), 2179.
- (10) Salentine, C. G. High-Field <sup>11</sup>B NMR of Alkali Borates. Aqueous Polyborate Equilibria. *Inorg. Chem.* **1983**, *22*, 3920.
- (11) Grace, T. M. *An Evaluation of Nonconventional Causticizing Technology for Kraft Chemical Recovery*; Progress Report (Project-3473-3); The Institute of Paper Chemistry, Jan 30, 1981.
- (12) Tran, H.; Sue, M.; Cameron, J.; Bair, C. M. Autoausticization of Smelt with Sodium Borates. *Pulp Pap. Can.* **1999**, *9*, 100.
- (13) Tran, H.; Mao, X.; Kochesfahani, S. H.; Bair, C. M. Occurrence of Borate Autoausticizing Reactions During Black Liquor Combustion. *TAPPI Technical Conference: Pulping & PCE&I*, Chicago, Fall 2003; Tappi Press: Atlanta, GA.
- (14) King, R. B. *Inorganic Chemistry of Main Group Elements*; VCH: New York, 1995; p 222.
- (15) *Inorganic Chemistry*, 34th ed.; Wiberg, N., Ed.; Academic Press: New York, 2001; p 128.
- (16) *CRC Handbook of Chemistry and Physics*, 82nd ed.; Lide, D. R., Ed.; CRC Press: Boca Raton, FL, 2001–2002; pp 4–85.
- (17) Wells, A. F. *Structural Inorganic Chemistry*, 4th ed.; Clarendon Press: Oxford, 1975; p 855.
- (18) Morey, G. W.; Merwin, H. E. Phase Equilibrium Relationships in the Binary System, Sodium Oxide-Boric Oxide with Some Measurements of the Optical Properties of the Glasses. *J. Am. Chem. Soc.* **1936**, *58*, 2248.
- (19) *NIST-JANAF Thermochemical Tables*, 4th ed.; Chase, M. W., Ed.; ACS: Washington, DC, AIPNIST: Woodbury, New York, 1998.
- (20) Grace, T.; Frederick, Wm. J. *Kraft Recovery Boilers*; Adams, T., Ed.; TAPPI Press: Atlanta, 1997; pp 163–179.
- (21) Frederick, W. J.; Way, J. D. Production of Hydrogen by Gasification of Spent Liquor. *AIChE Summer National Meeting*, Aug 1995; AIChE: New York, 1995.
- (22) Sricharoenchaikul, V.; Frederick, Wm. J.; Agrawal, P. Black Liquor Gasification Characteristics. 1. Formation and Conversion of Carbon-Containing Product Gases. *Ind. Eng. Chem. Res.* **2002**, *41*, 5640–5649.

Received for review January 23, 2004  
Revised manuscript received June 24, 2004  
Accepted July 21, 2004

IE049924B